6-10-2019

The (relative) insignificance of G revisited to include nanoparticles

Sungmin Youn

Desmond F. Lawler

The (relative) insignificance of G revisited to include nanoparticles

Sungmin Youn and Desmond F. Lawler

Submitted to JAWWA

July 2018

Revised and Re-submitted December 2018

The (relative) insignificance of G revisited to include nanoparticles

Corresponding Author: Sungmin Youn

Author 1 details:

Full name and credentials: Sungmin Youn, Ph.D.

Job title: Assistant Professor

Affiliation: Engineering Division, Marshall University, WV 25755, USA.

Mailing Address: 1676 Third Ave, Room 2207, Huntington, WV 25755 USA.

Preferred telephone number: 304 696 6475

Email address: youns@marshall.edu

Bio: Sungmin Youn has been a member of AWWA since 2015 and he is an assistant professor at Marshall University in West Virginia. He obtained his B.S. in Engineering at Calvin College in Grand Rapids, Michigan and his M.S. and Ph.D. from the University of Texas at Austin. This paper is based on his dissertation work.

Author 2 details:

Full name and credentials: Desmond F. Lawler, Ph.D.

Job title: Nasser I. Al-Rashid Chair in Civil Engineering and University of Texas Distinguished Teaching Professor

Affiliation: Dept of Civil, Architectural & Environmental Engineering, University of Texas, Austin, TX 78712 USA.

Mailing Address: Univ. of Texas; Mail Stop C1786; Austin, TX 78712

Preferred telephone number: 512 471 4595

Email address: dlawler@mail.utxas.edu

ABSTRACT

The collision efficiency functions, α(i,j), of two colliding particles for the three operative transport mechanisms in flocculation (Brownian motion, fluid shear, and differential sedimentation) were numerically calculated over a broad size range (including nanoparticles). All computations include the hydrodynamic force and van der Waals attraction, while the effects of electrical double layer repulsive forces were investigated by their exclusion or inclusion. Flocculation of nanoparticles should be extremely rapid if they are uncharged but will be dramatically reduced when substantially charged. For small neutral particles, α(i,j) values could be greater than one during fluid shear and differential sedimentation as van der Waals attraction outweighs the (negative) hydrodynamic effects. Overall, the results confirm the findings of an earlier paper, that Brownian motion is the dominant flocculation mechanism when at least one particle is small (<1 µm in diameter), fluid shear is only dominant when both particles are greater than 1 µm and the ratio of the two particle sizes is less than 10, and differential sedimentation is dominant in all other cases. Flocculators should be operated with low velocity gradient (G) values (in the range of 10 to 20 s^{-1}), with only sufficient mixing to keep particles in suspension, but proper particle destabilization is essential for effective flocculation.

INTRODUCTION

In 1992, Han and Lawler published the paper "The (relative) insignificance of G in flocculation"

in this Journal. The paper, which has been widely cited (218 times according to Google Scholar)

in the water treatment literature and in many theoretical treatises and papers related to other

industrial applications, noted that previous models of particle collisions did not account for the

hydrodynamic effects as particles approach one another and possibly collide. That paper and a

companion piece (Han & Lawler, 1991) explained that the curvilinear or short-range model that

accounted for those hydrodynamic effects resulted in substantial correction factors for the

traditional rectilinear or long-range model that ignored them. Those correction factors were

described as "α values," the fraction of collisions predicted to occur by the rectilinear model that

would occur according to the curvilinear model. These correction factors were particularly low

(in the range of 10^{-3} to 10^{-5}) for collisions by differential sedimentation (DS) and fluid shear (Sh)

when the larger particle in the two particle collision was fairly large and the smaller had a

diameter only a small fraction (0.1 or less) of the larger. Beyond the mathematics and computer

programming, the conclusion was that collisions by Brownian motion (Br) and DS were far more

prevalent than predicted by the traditional long-range model, and therefore that collisions by Sh

(i.e., the velocity gradient, G) were only dominant when both particles were above

approximately 1 μm in diameter and reasonably similar in size. In short, collisions by Sh were

far less important than previously thought (and hence the title). The authors concluded that G

values could be substantially less than in then-current standard designs—only enough to keep

particles in suspension where most collisions would occur by Br and DS. The short- and long-

range force models were examined in laboratory-scale experiments including both flocculation

by Li (1996) and precipitative flocculation by Nason and Lawler (2009). The short-range force

model was able to yield better predictions to the experimental data than the long-range force model. The short-range force model, updated from the original Smoluchowski number balance equation (1917) is written for a batch reactor as follows:

$$r_k^{Short-range} = \frac{dn_k}{dt} = \frac{1}{2}\alpha_{emp} \sum_{\substack{\text{all i and j} \\ Vi+Vj=Vk}} \gamma_{ij}^{tot} n_i n_j - \alpha_{emp} n_k \sum_{\text{all i}} \gamma_{ij}^{tot} n_i \qquad (1)$$

$$\gamma_{ij}^{tot} = \alpha_{ij}^{Br}\beta_{ij}^{Br} + \alpha_{ij}^{Sh}\beta_{ij}^{Sh} + \alpha_{ij}^{Ds}\beta_{ij}^{Ds}$$

where i, j and k are size classes of particles; n_i is the number concentration of i-sized particles (L^{-3}); V_i is the volume of a size i particle (L^3); and β_{ij} is the collision frequency function for particles of size i and j (L^3/T). The collision frequency function (β_{ij}), which is also known as the aggregation kernel, quantifies physical transport mechanisms (Brownian motion, fluid shear, and differential sedimentation) of the two colliding particles at long-range.

This paper addresses three limitations of Han and Lawler's original work. First, the previously developed α values were calculated only for conditions where the larger particle in the collision was one micrometer or greater. Because the use and production of engineered nanoparticles[1] are dramatically increasing, life-cycle pathways of nanoparticles in water and wastewater treatment (as well as in the natural environment) need to be addressed (Wiesner et al. 2006). The collision efficiency functions (α_{Br}, α_{Sh}, and α_{DS}) that account for hydrodynamic and interparticle forces have not previously been calculated for nanoparticles, and some of the short-range transport processes, in particular, might be significantly different for such small particles. To better understand the fate and transport of nanoparticles in water treatment and in the environment, α(i,j) values for these small particles were calculated.

---

[1] Nanoparticles are defined as natural, incidental, and manufactured materials that have external dimensions between 1 nm and 100 nm in at least one dimension and show different properties from their bulk materials (Foss Hansen et al. 2007).

Secondly, the previously reported α values were calculated under the assumption that the particles were well-destabilized by adsorption and charge neutralization in flocculation, so that the electric double layer (EDL) interactions between colliding particles would be negligible. In practice, however, perfect neutralization is not always achieved and particles are left with a smaller, but non-zero, surface charge. In addition, particle destabilization can also be achieved by compression of the diffuse layer (though never in a water treatment plant) or enmeshment in a precipitate, and in these cases, the surface charge is not negligible. For comprehensive understanding of particle destabilization, the EDL repulsive interactions were incorporated into the derivation of α.

Lastly, the existing collision efficiency values for fluid shear ($α_{Sh}$) need to be verified. Adler's global capture efficiency values (Adler 1981a) were obtained for only four particle size ratios, $λ$ = 0.1, 0.2, 0.5, and 1, where $λ$ is the size ratio of the smaller to larger particle in the two-particle collision. Han (1989) extrapolated and interpolated Adler's results to generate the collision efficiency functions for $λ$ values from near zero to 1. To generate $α_{Sh}$ values that are more accurate, Adler's trajectory analysis was performed under a wider and more closely spaced range of $λ$.

Several investigators (Chellam & Wiesner, 1993; Veerapaneni & Wiesner, 1996; Li & Logan, 1997; Serra & Logan, 1999) have criticized the Han and Lawler work because of the assumption that flocs are hard spheres that do not allow any water to flow through them. Real flocs, of course, are somewhat porous so that some water can flow through them; in that case, the true particle trajectories are likely to lie between those predicted by the long-range rectilinear model (all water flowing through the floc as if it were not there) and the short-range model (all water flowing around the floc as a solid sphere). Most authors who have confronted this question have

concluded that flocs should be considered as fractals, with the growth of flocs leading to a decrease in the fractal dimension. In a comprehensive experimental and modeling study, in which the model included the fractal nature of the flocs and a term for floc breakup, Zhang and Li (2003) concluded that the incorporation of the curvilinear model of Han and Lawler (1991, 1992) was quite superior to the use of the rectilinear model. Hence, the work reported herein takes the same hard-sphere approach as the previous work, recognizing that a fractal approach can be incorporated within that framework.

In this paper, we differentiate "micro-sized particles" (with a diameter larger than 1 μm) from "submicron-sized particles" (with a diameter smaller than or equal to 1 μm). This latter particle size range includes nanoparticles that are classified by the standard definition given in footnote 1. Mathematical derivations are explained in the Methods section. The results from the numerical computations are presented as two separate parts in the Results section to describe α in the absence and presence of the EDL repulsion.

METHODS

Collision Efficiency Function for Brownian Motion (α_{Br}). By definition, stability (W) is the ratio of the aggregation rate in the absence of repulsive interactions between particles to the aggregation rate in the presence of repulsive interactions (Stumm & Morgan 1996). For Brownian collisions, Smoluchowski's diffusion equation (1917) gives the solution to the aggregation rates in the absence of repulsive interaction, while Fuchs's diffusion equation (1934) provides the solutions in the presence of repulsive interaction. Stability (W) is the reciprocal of the collision efficiency function (α_{Br}) for Brownian motion (Stumm & Morgan 1996). Spielman (1970) derived the stability (W) with hydrodynamic and the EDL repulsive interaction between two particles as shown below.

$$W = \left(1 + \frac{a_2}{a_1}\right) \int_{1+\frac{a_2}{a_1}}^{\infty} \frac{D_{12}^{\infty}}{D_{12}} \frac{\exp\left(\frac{V_{PE}}{kT}\right)}{s^2} \, ds = \frac{1}{\alpha_{Br}} \qquad (2)$$

where a_1 and a_2 are the radii of two colliding particles ($a_1 \geq a_2$ by convention), D_{12} is the relative diffusion coefficient, D_{12}^{∞} is the diffusion coefficient at infinite separation, V_{PE} is the total interparticle potential energy (*i.e.*, DLVO energy), k is Boltzmann's constant, and T is temperature in Kelvin. To calculate the DLVO energy, the linearized Poisson-Boltzmann equation with constant potential and the retarded vdW equation that accounts for dipole-dipole interactions and their propagation in water were used (Elimelech et al. 1998). Han (1989) solved the hydrodynamic portion of the equation (*i.e.*, D_{12}^{∞}/D_{12}) using Jeffrey and Onishi's (1984) resistance and mobility tensor solutions, and then numerically solved the integral to acquire Brownian collision efficiency functions for the case with vdW only (i.e., no EDL). In this research, Han's method was utilized to solve Spielman's equation (Eqn 2) in the presence of hydrodynamic, vdW, and EDL forces.

Collision efficiency function for differential sedimentation (α_{DS}). For collisions by differential sedimentation, Han and Lawler (1981) used Batchelor's equation (1982) to convert Jeffrey and Onishi's (1984) resistance and mobility tensor solutions to velocities of two settling particles. The relative trajectory of the smaller particle with respect to the larger particle is depicted in a polar coordinate system shown in Figure 1.
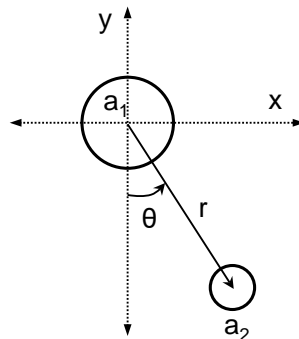
Figure 1. Schematic of two particles in differential settling (adapted from Han and Lawler 1991)

From a Lagrangian point of view, the origin of the polar coordinate is at the center of the larger particle. The following differential equation gives the distance (r) between the two particles as a function of the angle (θ) between the particles during differential sedimentation. Given an initial location of the two approaching particles,

$$\frac{dr}{d\theta} = s \frac{-\cos\theta[L(s,\lambda)]U_{s12} + \frac{D_{12}}{kT}[G(s,\lambda)]\nabla\phi_{12}}{[M(s,\lambda)](\sin\theta)U_{s12}} \tag{3}$$

where s is the center-to-center separation distance normalized by the average of two particle radii (*i.e.*, s=2r/(a$_1$+a$_2$)), L(s, λ) and M(s, λ) are the hydrodynamic correction terms to a particle's settling velocity, G(s, λ) represents the hydrodynamic correction term to the diffusivity coefficient, U$_{s12}$ is differential settling velocity, and ∇φ$_{12}$ represents the gradient of the total interparticle potential energy (*i.e.*, DLVO energy). Solving the above equation, the distance and the angle of the smaller particle is determined relative to the center of the larger particle (the origin). Details of mathematical derivations and computational conditions are provided by Han (1989) and Han and Lawler (1991). In this research, this first order nonlinear differential equation was solved numerically using ODE Solvers in Matlab.

In trajectory analysis, open trajectories mean that particles miss each other during the course of their interaction, whereas closed trajectories mean that particle collisions occur (*i.e.*, the normalized separation distance between two particles, s, is equal to 2). The collision efficiency function (α$_{DS}$) is the ratio of the critical cross-sectional area that leads to closed trajectories in the presence of interparticle forces (i.e., the short range or curvilinear model) to the critical cross-

sectional area that leads to closed trajectories in the absence of those external forces (the long range or rectilinear model), as shown in Figure 2.
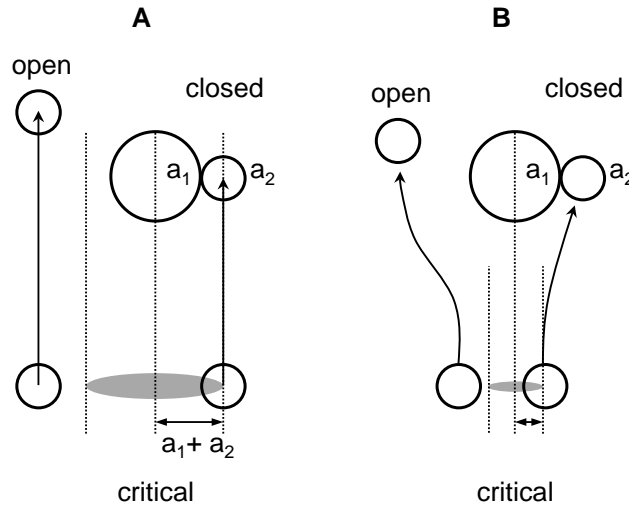
Figure 2. Critical areas in the absence of interparticle forces (A) and in the presence of interparticle forces (B). (Adapted from Benjamin and Lawler 2013)

Collision efficiency function for a linear shear flow (α_{Sh}) Adler presented the global capture efficiencies in collisions of two unequal-sized particles in a linear shear fluid (1981a, 1981b, 1981c, 1981d) by improving van de Ven and Mason's derivation (1976a, 1976b). To calculate the collision efficiency functions for particles in linear shear flow, Adler's trajectory analysis was performed in this research with the inclusion of the interparticle interactions (vdW and EDL). The relative trajectory of two particles moving at different velocities due to a linear shear flow in polar coordinates is schematized in Figure 3.
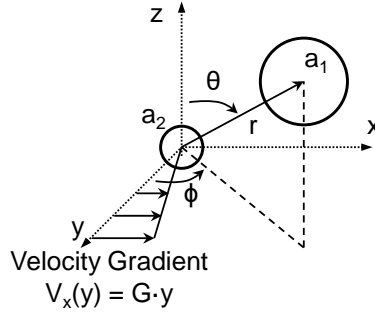
Figure 3. Schematic of two particle interactions in a linear shear flow. (Adapted from Tandon and Diamond 1997)

The origin of the polar coordinate is at the center of particle 2. The coordinates of particle 1 are θ (the angle between particle 1 and the z-axis), ϕ (the angle between particle 1 and the y-axis), and r (the center to center distance between the two particles). Three first order differential equations describe the changes in r, θ, and ϕ with respect to time, t; as follows (Adler, 1981b):

$$\frac{dr}{dt} = G \cdot r(1 - A) \sin^2 \theta \sin \phi \cos \phi + F \tag{4}$$

$$r\frac{d\theta}{dt} = (1 - B) \sin \theta \cos \theta \sin \phi \cos \phi \tag{5}$$

$$r \sin \theta \frac{d\phi}{dt} = G \cdot r \sin \theta \left(\cos^2 \phi - \frac{B}{2} \cos 2\phi \right) \tag{6}$$

where G is a linear velocity gradient, A and B are dimensionless hydrodynamic correction factors (Adler 1981b, 1981c) that depend on λ and r, and F is the total interparticle force (*i.e.*, the sum of vdW and EDL forces). Tandon and Diamond (1997) devised simpler hydrodynamic fitting functions that yield less than 2% error from the exact values of Adler (1981a) and Batchelor and Green (1972); these simpler functions were used in this work to reduce the computational burden.

RESULTS: COLLISION EFICIENCY IN THE ABSENCE OF EDL REPULSION

8

Collision Efficiency Function for Brownian Motion (α_{Br}). First, α was calculated under the assumption of complete particle destabilization where the EDL repulsive forces are negligible. Using two different values for the Hamaker constant (A_H) (10 and 50 k_BT, which are equivalent to 4.11E-20 and 2.06E-19 J, respectively), the collision efficiency functions under Brownian motion (α_{Br}) for various particle sizes were calculated as shown in Figure 4. These values of the Hamaker constants were chosen based on the work of Israelachvili (2011) considering inorganic, organic, and metal particles in water. The computed Brownian collision efficiencies for A_H of 10 k_BT (Figure 4A) are consistent with the previously reported values (Han 1989, Han et al. 1997), except for the two additional lines for $a_1 = 0.5$ and 5 nm which are the new results of this study. When A_H was raised to 50 k_BT, the lines in the graph shifted upward (Figure 4B), as expected with this increased van der Waals attraction. In this figure (and subsequent figures), the points shown were calculated directly from the numerical analysis, but the lines represent polynomial fits of those points. The polynomial fitting equations for each figure under the conditions of complete charge neutralization are tabulated in the Appendix.

The collision efficiency, α_{Br}, decreased as the size ratio (λ) in the two-particle collision increased when the size of the bigger particle (a_1) was fixed. This result reflects the fact that particle diffusivity decreases with increasing size. Similarly, α_{Br} decreased as a_1 increased when λ was constant. However, even at the high value of the Hamaker constant, α_{Br} values never exceeded or became unity at any particle sizes or size ratios in any cases due to the hydrodynamic (viscous) forces that act against collisions.
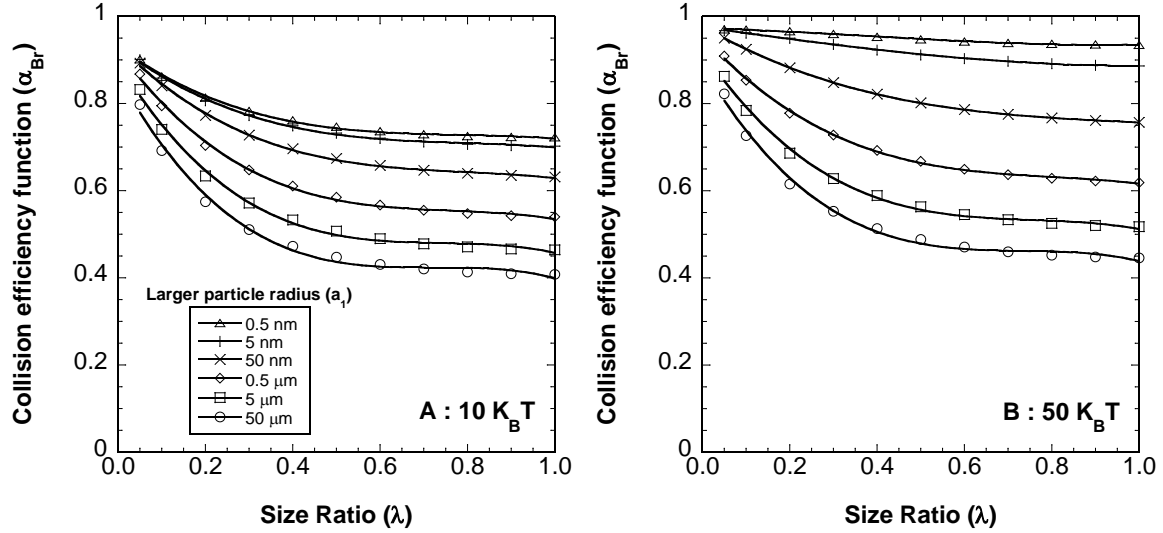
Figure 4. The collision efficiency functions in Brownian motion under two different Hamaker constant values.

Collision Efficiency Function for Differential Sedimentation (α_{DS}). The calculated collision efficiency functions of differential sedimentation (α_{DS}) in the absence of the EDL repulsion are presented in Figure 5. A dimensionless parameter, N_g, is used to incorporate all of the influencing variables in differential sedimentation transport (Han and Lawler 1992; Benjamin and Lawler 2013):

$$N_g = \frac{3A_H}{\pi(\rho_P - \rho_L)g{a_1}^4} \tag{7}$$

where g is the gravitational constant, and ρ_P and ρ_L are the densities of the particles and fluid, respectively. Figure 5 shows α_{DS} for $\log(N_g)$ values from -6 to 6. When α_{DS} values were first reported by Han and Lawler, trajectory analysis was performed only up to $\log(N_g) = 1$, which was sufficient to deal with the relevant particle sizes at the time of study. At that time, it was thought that the upper limit of α_{DS} was unity when $\log(N_g) > 1$.

However, Figure 5 shows that α_{DS} gradually ascends as $\log(N_g)$ is increased and eventually exceeds unity. This result means that the balance between vdW attraction (which acts to pull

10

particles together) and hydrodynamic effects (which drive particles apart) favors the vdW

attraction in differential sedimentation when the log Ng value exceeds 1. That is, as a larger

particle falls, a smaller particle below can be drawn toward and collide with the larger particle,

even if the smaller particle starts outside the area associated with the critical trajectory in the

long-range model depicted in Figure 2. For log Ng to exceed 1, the larger particle itself is quite

small, so the settling velocities are small, the hydrodynamic effects are small, and the time for

one particle to pass another is large; thus vdW attraction can cause the particles to come together.
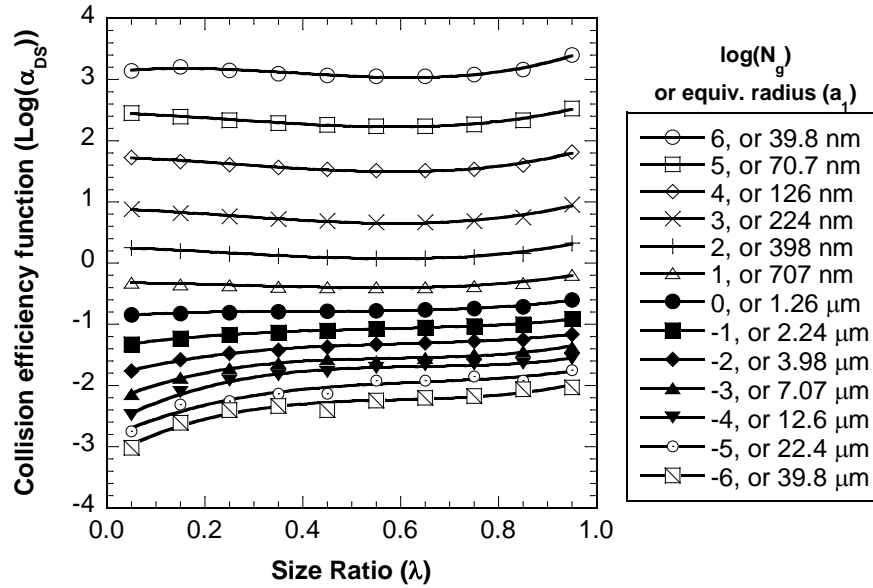
Figure 5. The collision efficiency functions in differential sedimentation. (The calculations were

performed with A_H = 10 k_BT, ρ_P = 2.6 g/cm^3, and ρ_L = 1 g/cm^3 and the larger particle radius

varied as shown in the legend but any combination of values that leads to the same N_g value

leads to the same result.)

Collision Efficiency Function for Fluid Shear (α_{Sh}).   The calculated collision efficiency

values in a linear shear flow (α_{Sh}) in the absence of the EDL repulsion are presented in Figure 6.

Similar to differential sedimentation, a dimensionless number, H_A, incorporates all of the controlling variables in fluid shear transport (Adler 1981a):

$$H_A = \frac{A_H}{144\pi\mu a_1{}^3 G} \qquad (8)$$

where G is the velocity gradient and μ is the absolute viscosity of the fluid.

Figure 6 shows slightly different α_{Sh} values than those reported by Han and Lawler (1992). As explained earlier, Han and Lawler interpolated and extrapolated from Adler's work, which was performed at only four λ values whereas this research was performed using more closely spaced λ values between 0.1 and 1. For values of $\log H_A \leq -4$, the results here confirm Han and Lawler's conclusion (1992) that collisions with particles that are much smaller ($\lambda < 0.4$) rarely occur. What is new and remarkable is that, as H_A and λ increase, α_{Sh} values become greater than unity (i.e., $\log \alpha_{Sh} > 0$). As shown above for differential sedimentation, the vdW attraction dominates at the submicron-scale in short-range transport by fluid shear, and sub-micron particles have a collision efficiency greater than one.
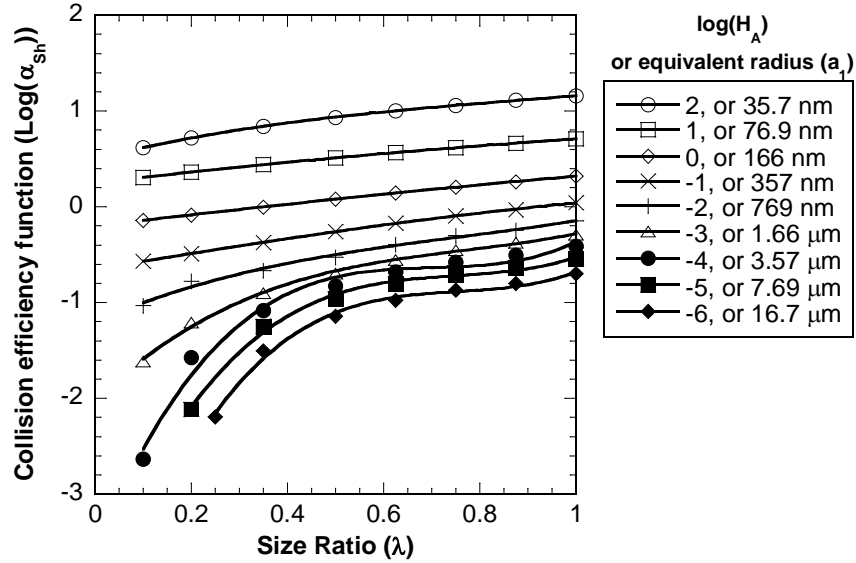
Figure 6. The collision efficiency functions in fluid shear (The calculations were made with A_H = 10 $k_B T$, G = 20 s^{-1}, and μ = 0.01 g/cm-s and the larger particle radius varied as shown in the legend but any combination of values that leads to the same H_A value leads to the same result.)

RESULTS: COLLISION EFICIENCY IN THE PRESENCE OF EDL REPULSION

Collision Efficiency Function for Brownian Motion (α_{Br}). When a constant surface potential (ζ potential) of -25 mV in the ionic strength of 1 mM was integrated into the identical conditions of Figure 4A (where A_H was 10 $k_B T$), α_{Br} was lowered substantially by the presence of the EDL repulsion, as shown in Figure 7. The degree of α_{Br} reduction due to the EDL repulsion increased dramatically as the size of the larger particle (a_1) in the collision increased. For any particle with a radius greater than 50 nm, α_{Br} was negligible (i.e., near zero) in the presence of the constant surface potential of -25 mV, meaning that few, if any, collisions caused by Brownian motion between a particle of 50 nm (or larger) and any smaller particle would actually happen and allow a floc to be formed. This result highlights the importance of particle destabilization by proper chemical addition in the rapid mix tank in water treatment plants.

The heights of interaction energy barriers (*i.e.*, DLVO energy barrier) due to the EDL repulsion are strongly influenced by the sizes of the two interacting particles (Benjamin & Lawler 2013). When the size of the larger particle (a_1) in the collision gets larger, particle diffusion coefficients decrease while the DLVO energy barrier rises; conversely, as a_1 gets smaller, diffusion coefficients increase while the DLVO energy barrier falls. For this reason, collisions between smaller particles through short-range transport were less hindered by the presence of the EDL repulsion.
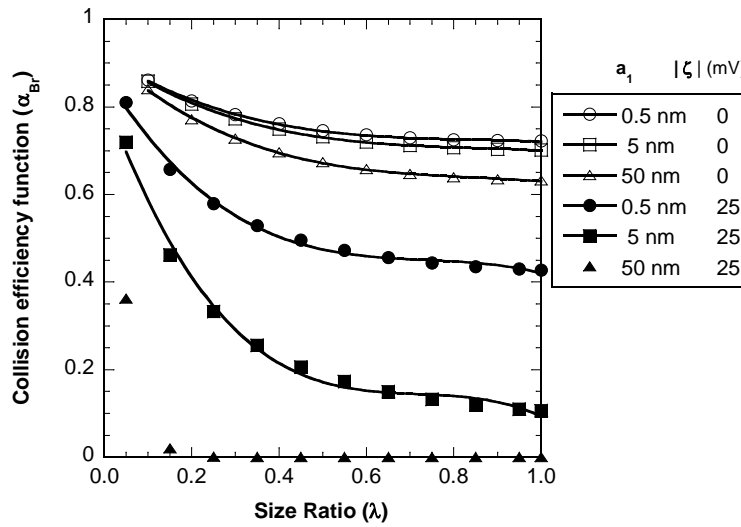
Figure 7. α_{Br} in the presence/absence of the constant surface potential of -25 mV

The influence of surface potential and ionic strength on collision efficiency functions are shown in Figure 8. Ionic strength is correlated to specific conductivity of water (e.g., 1 mM KCl is approximately 147 µS/cm). The results in Figure 8A and 8B are as would be expected qualitatively: α_{Br} increases with increasing ionic strength (or conductivity) and decreasing surface potential. These trends agree with Han and Lee's (2002) experimental results. In the presence of the EDL, α_{Br} is a function of the ionic strength, the surface potential, and the colliding particle sizes.
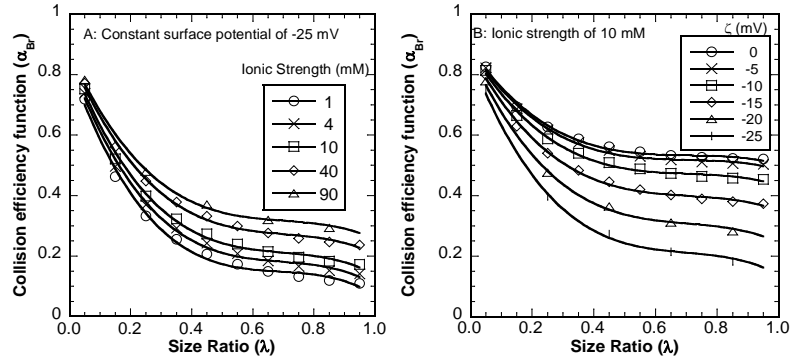
Figure 8. α_{Br} for charged particles with A) various ionic strengths and B) various surface

potentials for $a_1 = 5$ nm

Collision Efficiency Function for Differential Sedimentation (α_{DS}). With the constant

surface potential of -25 mV, particle trajectories in differential sedimentation were simulated for

four distinct a_1 values ($a_1 = 5$ nm, 500 nm, 5 µm, and 50 µm, which are equivalent to $\log(N_g) =$

5.6, 1.6, -2.4, and -6.4, respectively, under the same conditions that were assumed in producing

Figure 5). As expected, the presence of the EDL repulsion reduces α_{DS}. When a_1 was smaller

than or equal to 5 µm with any size of a_2, no collisions were predicted to occur (*i.e.*, $\alpha_{DS} = 0$) at

this surface potential. That is, below some size for the larger particle, two approaching particles

never collide by differential sedimentation in the presence of the EDL repulsion.

More interestingly, at the nano/submicron-scale ($a_1 < 0.5$ µm), simulated trajectories showed that

two settling particles never collide in the course of settling, but particles orbit each other with a

fixed separation distance (at the secondary minimum of the DLVO energy curve). This

phenomenon, the formation of so-called "secondary doublets," has been discussed for particle

collisions in a linear shear flow by Adler (1981b) and Van de Ven (1989) and in differential

sedimentation by Melik and Fogler (1984). The results of this trajectory analysis suggest that the

interparticle forces dictate the transport behavior more significantly than the settling forces for

submicron-sized particles. At the submicron-scale, the differential settling force is simply not

15

sufficient to overcome the primary DLVO energy barrier. This phenomenon, while intellectually interesting, is not particularly important in water treatment.

When a_1 was greater than 50 µm, direct particle collisions were observed occasionally even in the presence of the constant surface potential of -25 mV. The settling force (or momentum) at these particles sizes was large enough to overcome the DLVO energy barriers. When the direct collisions occurred at these particle sizes, α_{DS} was substantially lowered in comparison to the non-EDL case, and the maximum values of α_{DS} were estimated to be on the order of 10^{-4}. However, it was not feasible to create a generalized graph of α_{DS} with polynomial fittings in the presence of a constant surface potential. Several influencing variables that control α_{DS} values in numerical trajectory analysis are not incorporated into the dimensionless number, N_g; those variables include ionic strength and the magnitude of surface potential. To get an accurate value of α_{DS}, each specific physical and chemical condition requires separate numerical computation. These results again point to the criticality of excellent particle destabilization in drinking water treatment.

Collision Efficiency Function for fluid shear (α_{Sh}). Because Adler (1981a) already presented the influence of the EDL repulsion on global capture efficiencies regarding micro-sized particles in a shear field, the main focus of this paper is the extension to submicron-sized particles under the influence of the EDL. When the surface potential of -25 mV was included in the trajectory analysis, the critical cross-sectional area that can result in particle collisions is effectively minimized. At the nano/submicron-scale, the external shear force acting on the particles is unable to overcome the DLVO energy barrier, and particle transport is primarily governed by the interparticle forces. As a result, the presence of the EDL hinders particle collision to a greater extent for submicron-sized particles than micro-sized particles. Just as for

α_{DS} in the presence of the EDL, the polynomial fits for α_{Sh} as a function of the sizes and the size ratio of the two colliding particles could not be easily generated in the presence of the EDL. The dimensionless number, H_A does not include all of the factors that affect α_{Sh}. For each specific physiochemical condition, individual trajectory analysis would need to be performed.

Collision Rates in the Absence and Presence of EDL repulsion for Sub-micrometer Particles

To visualize the relative importance of the three transport mechanisms in flocculation for a submicron-sized particle with a wide range of particle sizes, the calculated collision efficiency functions (α) are combined with the collision frequency functions (β) and illustrated in Figure 9. Figure 9 displays the corrected collision frequency values ($\gamma = \alpha*\beta$) for the three transport mechanisms of two-particle collisions considering various surface potentials and otherwise fixed conditions ($A_H = 10$ k_BT, density = 2.4 g/cm^3, and G = 20 s^{-1}); each part of the figure is for one transport mechanism. The diameter of one particle in the collision (d_1) was fixed at 200 nm while the diameter of the second particle in the collision (d_2) was varied; the scale in all three parts of the figure is the same to ease comparison.

The corrected collision frequency values ($\alpha*\beta$) showed no clear differences among the surface potentials of 0, -10, and -20 mV for both Sh and DS transport (Figure 9, Parts B and C). When the surface potential was increased to -30 mV, however, particle collisions were not observed at all (α_{DS} and α_{Sh} became 0). These results, showing little to no effect of surface potential at low values and a sudden drop to no possible collisions at a critical value, are in agreement with results reported by Melik and Fogler (1984). For the conditions depicted in Figure 9, the critical potential was close to ~30 mV.

The results for collisions by Brownian motion (Figure 9A) are considerably different. The corrections to the long range model ($\beta(i,j)$) are relatively mild when considering the hydrodynamic interactions and van der Waals attraction alone (the 0 EDL case) and only slightly stronger with $\zeta = -10$ mV; that is, the collision rates for all particles colliding with the 0.2 μm diameter particle under consideration are reduced by less than one order of magnitude.

However, with a surface potential of -20 mV, a substantial reduction in the corrected collision frequency for Br transport (Figure 9A) was observed, while there was no change at that potential for Sh and DS (Figure 9, parts B and C). Taken together, these results suggest that, for (perhaps) a small window of surface potentials (in the range of -20 to -30 mV in this example) and a small window of particle sizes, particle collisions for small particles are more likely to occur by shear and differential sedimentation than by Brownian motion. However, even in that range where the α values for Sh and DS are greater than one, the corrected collision frequency function is at a low value (in the range of 10^{-12} cm^{3}s^{-1}) for Sh, which is the dominant mechanism.

A. Brownian Motion

β_{Br}

$\alpha\beta_{Br}$ (ζ=0)

$\alpha\beta_{Br}$ (ζ=-10mV)

$\alpha\beta_{Br}$ (ζ=-20mV)

B. Shear

$\alpha\beta_{Sh}$
(all three ζ potentials)

β_{Sh}

C. Differential Sedimentation

$\alpha\beta_{DS}$
(all three ζ potentials)

β_{DS}

Collision Frequency Function (cm^{3}s^{-1})

Particle Diameter (d$_2$ in μm)
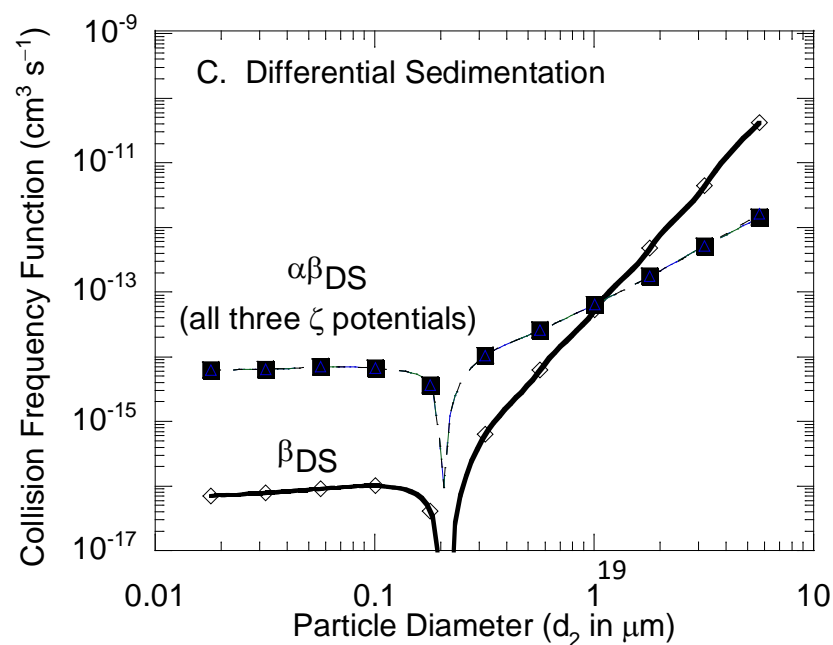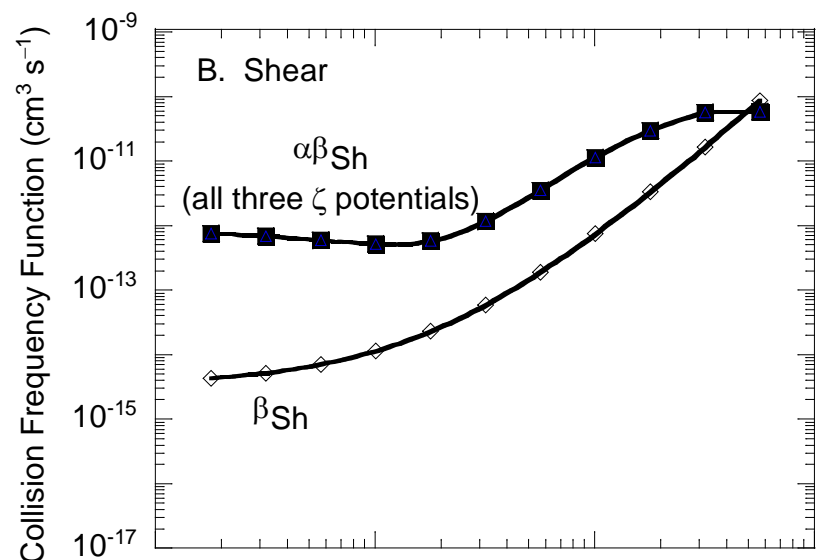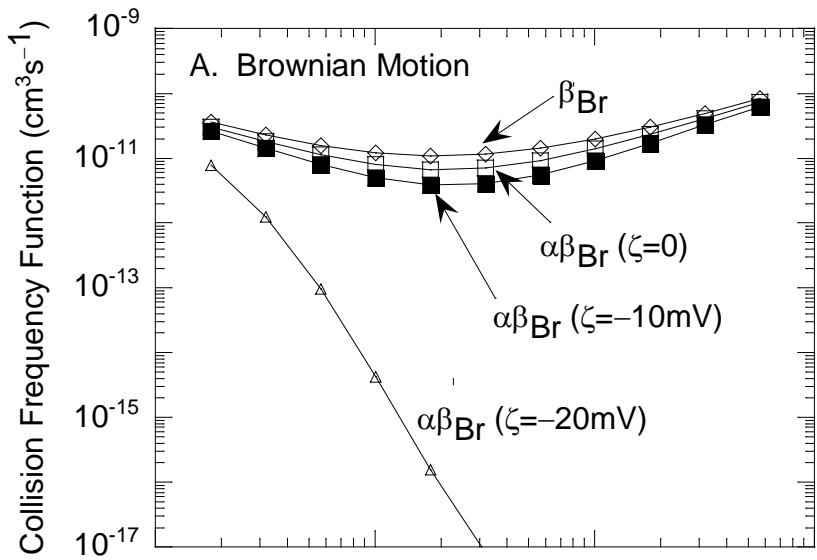
Figure 9. Total Collision frequency function for the three transport mechanisms (A - differential sedimentation, B - fluid shear, and C - Brownian Motion) for varying surface potentials in the range of -20 to 0 mV. The diameter of the first particle (d_1) in collision is fixed at 200 nm while the diameter of the second particle (d_2) varies. For $\zeta = -30$ mV and any more negative values, the total collision frequency function ($\alpha\beta$) is zero for all three transport mechanisms.

In the well-destabilized scenario (for $\zeta = 0$ and -10 mV), Brownian motion is the dominant transport for particle collisions between the 200 nm sized particle and particles of any size. Differential sedimentation (gravity, g) and linear shear flow (velocity gradient, G) are not important in flocculation in this case. This result is consistent with the conclusion made by Han & Lawler in 1992.

The results of these numerical calculations in the presence of EDL illuminate the importance of particle destabilization in water treatment. Most turbidity in water is caused by sub-micron sized particles. What both this paper and the previous Han and Lawler (1992) paper indicate is that sub-micron particles flocculate almost exclusively by Brownian motion. Mixing intensity is relatively less critical for turbidity removal in water treatment than other parameters such as a coagulant dose and pH (i.e., particle destabilization).

CONCLUSION

Flocculation, the conversion of a large number of small particles into a smaller number of larger particles, is a critical process in conventional surface water treatment. The current paper extends the earlier work of Han and Lawler (1991, 1992) by considering smaller particles and by considering particles that are not completely destabilized by charge neutralization.

The first conclusion is consistent with the earlier paper: when particles are completely destabilized by charge neutralization, particle collisions are dominated (1) by Brownian motion when one of the particles is less than one micrometer and the other is any size, (2) by differential sedimentation when both particles are greater than one micrometer and substantially different in size, and (3) by fluid shear only when both particles are greater than one micrometer and relatively similar in size (within a factor of ten or so). These results support the idea first proposed by Han and Lawler (1992) and later supported by Kawamura (2000). On page 114 of his book, Kawamura suggested that flocculators can and should be designed with low mixing intensity (for example, G of 12 s^{-1} for 45 minutes), just sufficient to keep the particles in suspension and allow the dominant collisions by Br and DS to occur. In addition, these results are in good agreement with laboratory-scale experiments for flocculation of silver nanoparticles (Youn, 2017).

The new finding in this paper, under the condition of charge neutralization, is that collisions between two small particles can occur far more frequently than previously thought by Sh and DS because the α values can be greater than one, and in some cases, a few orders of magnitude greater than one; nevertheless, Brownian motion still exhibits the highest collision frequency function.

However, when sub- micrometer particles have a substantial surface charge, they are far more difficult to flocculate, according to the modeling done in this paper. Their small size makes them more susceptible to the influence of short-range forces—the hydrodynamic interactions, van der Waals attraction, and electrostatic repulsion. With the existence of a surface potential greater (in absolute value) than 20 mV, nanoparticles are very stable and will not easily be removed from drinking water. Surprisingly, however, the modeling suggests that a relatively broad range of

21

surface potentials (with absolute values less than approximately 20 mV) can lead to effective flocculation of sub-micrometer particles. Nevertheless, optimum coagulation conditions in water treatment encompass both a coagulant dose and pH that can vary with water quality and temperature. Although effective destabilization encompasses a fairly wide range of surface potentials, at least for sub-micrometer particles, particle destabilization is a critical process in water treatment. Both engineered and natural nanoparticles can be expected to be removed to a very high degree in well-operated water treatment plants.

Lastly, the mathematical results presented in this paper improve the quantitative understanding of water treatment as well as the environmental fate and transport of engineered nanoparticles. Many scholars have suggested that engineered nanoparticles in aqueous systems are likely to aggregate to form micro-sized clusters (Hotze *et al.*, 2010). The mathematical models presented in this paper numerically support their argument with respect to nanomaterial aggregation processes.

Acknowledgement

References

Adler, P. M., 1981a. Heteroflocculation in shear flow. Journal of Colloid and Interface Science, 83(1), 106-115.

Adler, P. M., 1981b. Interaction of unequal spheres: I. Hydrodynamic interaction: colloidal forces. Journal of Colloid and Interface Science, 84(2), 461-473.

Adler, P. M., 1981c. Interaction of unequal spheres: II. Conducting spheres. Journal of Colloid and Interface Science, 84(2), 475-488.

Adler, P. M., 1981d. Interaction of unequal spheres: III. Experimental. Journal of Colloid and Interface Science, 84(2), 489-496.

Batchelor, G. K., 1982. Sedimentation in a dilute polydisperse system of interacting spheres. Part 1. General theory. Journal of Fluid Mechanics 1982, 119: 379-408.

Batchelor, G.K., & Green, J.T., 1972. The hydrodynamic interaction of two small freely-moving spheres in a linear flow field. Journal of Fluid Mechanics, 56(02): 375-400.

Benjamin, M. M., & Lawler, D. F., 2013. Water quality engineering: physical/chemical treatment processes. John Wiley & Sons: New Jersey.

Chellam, S. & Wiesner, M. R., 1993. Fluid-Mechanics and Fractal Aggregates. Water Research, 27 (9), 1493-1496.

Elimelech, M.; Gregory, J.; & Jia, X., 1998. Modeling of aggregation processes. In Particle deposition and aggregation: measurement, modeling and simulation. Butterworth-Heinemann: Woburn, MA., pp 157-199.

Foss Hansen, S., Larsen, B. H., Olsen, S. I., & Baun, A., 2007. Categorization framework to aid hazard identification of nanomaterials. Nanotoxicology, 1(3), 243-250.

Fuchs, V.N., 1934. Über die stabilität und aufladung der aerosole. Zeitschrift für Physik, 89(11-12): 736-743.

Han, M., 1989. Mathematical modeling of heterogeneous flocculent sedimentation (Doctoral dissertation, University of Texas at Austin).

Han, M., Lee, H., Lawler, D. F., & Choi, S., 1997. Collision efficiency factor in brownian flocculation (αBr) including hydrodynamics and interparticle forces. Water science and technology, 36(4): 69-75.

Han, M., & Lawler, D.F., 1991. Interactions of two settling spheres: Settling rates and collision efficiency. Journal of Hydraulic Engineering, 117(10), 1269-1289.

Han, M., & Lawler, D.F., 1992. The (relative) insignificance of G in flocculation. Journal (American Water Works Association), 84(10), 79-91.

Han, M., & Lee, H., 2002. Collision efficiency factor in Brownian flocculation (α Br): Calculation and experimental verification. Colloids and Surfaces A: Physicochemical and Engineering Aspects, 202(1): 23-31.

Hotze, E. M., Phenrat, T., & Lowry, G. V. (2010). Nanoparticle aggregation: challenges to understanding transport and reactivity in the environment. Journal of environmental quality, 39(6), 1909-1924.

Israelachvili, J.N., 2011. Intermolecular and surface forces. Academic press.

Jeffrey, D. J., & Onishi, Y., 1984. Calculation of the resistance and mobility functions for two unequal rigid spheres in low-Reynolds-number flow. Journal of Fluid Mechanics, 139: 261-290.

Kawamura, S., 2000. Integrated design and operation of water treatment facilities. John Wiley & Sons.

Li, J., 1996. Rectilinear vs. curvilinear models of flocculation: Experimental tests (Doctoral dissertation, University of Texas at Austin).

Li, X. Y. & Logan, B. E., 1997. Collision Frequencies between Fractal Aggregates and Small Particles in a Turbulently Sheared Fluid. Environmental Science & Technology, 31 (4), 1237-1242.

Melik, D.H. and Fogler, H.S., 1984. Gravity-induced flocculation. Journal of colloid and interface science, 101(1), pp.72-83.

Nason, J.A. and Lawler, D.F., 2009. Modeling particle-size distribution dynamics during precipitative softening. Journal of Environmental Engineering, 136(1), pp.12-21.

Serra, T. & Logan, B. E., 1999. Collision Frequencies of Fractal Bacterial Aggregates with Small Particles in a Sheared Fluid. Environmental Science & Technology, 33 (13), 2247-2251.

Smoluchowski, M., 1917. Verscheiner Mathematischen Theorie der Koagulations-Kinetic Kolloider Losungen. Z. Physik Chem. (Leipzig), 92: 129-168.

Spielman, L. A., 1970. Viscous interactions in Brownian flocculation. Journal of Colloid and Interface Science. 33(4): 562-571.

Stumm, W., & Morgan, J.J., 1996. Chemical equilibria and rates in natural waters. In Aquatic chemistry. John Wiley & Sons: New York, p.1022.

Tandon, P., & Diamond, S. L., 1997. Hydrodynamic effects and receptor interactions of platelets and their aggregates in linear shear flow. Biophysical journal, 73(5): 2819-2835.

Van de Ven, T. G. M., & Mason, S. G., 1976a. The microrheology of colloidal dispersions: IV. Pairs of interacting spheres in shear flow. Journal of Colloid and Interface Science, 57(3): 505-516.

Van de Ven, T. G. M., & Mason, S. G., 1976b. The microrheology of colloidal dispersions: V. Primary and secondary doublets of spheres in shear flow. Journal of Colloid and Interface Science, 57(3): 517-534.

Van de Ven, T.G., 1989. Colloidal hydrodynamics. Academic Press: San Diego, CA.

Veerapaneni, S. & Wiesner, M. R., 1996. Hydrodynamics of Fractal Aggregates with Radially
  Varying Permeability. Journal of Colloid and Interface Science, 177 (1), 45-57.

Wiesner, M.R., Lowry, G.V., Alvarez, P., Dionysiou, D., & Biswas, P., 2006. Assessing the risks
  of manufactured nanomaterials. Environmental science & technology, 40(14), 4336-4345.

Youn, Sungmin, 2017. Quantitative Understanding of Nanoparticle Flocculation in Water
  Treatment, Austin TX, The University of Texas at Austin.

Zhang, J. J., & Li, X. Y., 2003. Modeling particle-size distribution dynamics in a flocculation
  system. AIChE Journal, 49(7), 1870-1882.